Basic Study on Short Distance Landing Control with Reverse Thrust of Variable Pitch Propeller for Fixed Wing Electric Aircraft

Pinzhe Feng[1], Yuto Naoki[1], Kota Fujimoto[1], Kentaro Yokota[2], Sakahisa Nagai[1], Hiroshi Fujimoto[1]
[1]*The University of Tokyo,* Kashiwa, Japan
[2]*Japan Aerospace Exploration Agency,* Sagamihara, Japan
Corresponding author's e-mail: hyou.hintetsu24@ae.k.u-tokyo.ac.jp

***Abstract*—In the aviation industry, a short landing distance for aircraft is quite important which may broaden the usage of it. For a propeller-driven aircraft, variable pitch propeller (VPP) is widely used to create reverse thrust as air brake. However, because of the complexity of VPP mechanism and low controllability of internal combustion engine, a hydraulic type VPP may not allow a large range variation of the pitch angle. On the other hand, regarding electric aircrafts, its controllability is approximately 100 times higher than conventional engine thanks to a fast response of electric motor. This characteristic may make it possible to use wider range of pitch angle to make larger thrust for shorter landing distance than usual. In this paper, a basic study of the feasibility of using VPP to achieve the short landing distance control for a fixed wing electric aircraft is conducted. A pitch angle transition for opposite direction as to a conventional transition is proposed for the larger reverse thrust. An experiment is conducted to obtain a static characteristic of VPP for the larger thrust. To the end, simulations are conducted to verify the proposed pitch angle transition for shorter landing distance with parameter identified in experiments, and it is confirmed that the proposed method can reduce the landing distance up to $30\,\%$ compared to the conventional pitch transition.**

***Index Terms*—Electric aircraft, variable pitch propeller, reverse thrust, pitch placement, thrust coefficient.**

I. Introduction

With the growing environmental awareness of the society, the electrification of mobilities receives more attentions and electric aircraft (EA) becomes one of the main area in the electrification research. An all electric aircraft is powered by electric motors and it may have several advantages compared to a usual internal combustion engine aircraft.

- The greenhouse gas emission of EA is relatively lower than usual aircraft [1].
- The response time of an electric motor to generate torque is 100 times faster than engine which may make EA to be highly controllable and much more safer than usual aircraft [2].
- Under particular situation, electric energy may be regenerated as a result of the reversal of counter torque [3].
- Motor torque can be estimated accurately using a lot of means [4].

However, the low output energy density and short cruising distance due to the limitation of batteries restrict the development of EA.

Taking both advantages and disadvantages into consideration, several research field is established. Focusing on the extension of the cruising distance for EA, the research of the development of new high energy density generator for EA [5] or the regeneration of electric energy during the aviation using the pitch angle control of propeller [6] have been conducted. Besides, electric unmanned aerial vehicles (eUAVs) are also widely used and studied, which is also known as electric vertical take-off and landing aircraft (eVTOL). It is expected to aid the urban material transportation [7] or even daily transportation for people [8] because of the vertical take off ability even in urban area. Even in the research field of eVTOL, there are several different research directions such as the altitude control of a multirotor type drone [9], or the optimization of a tilt-wing type eVTOL [10]. However, because of the large amount of energy consumption while take off and landing, it may not be able to have a long cruise distance and a relative small payload ability.

Further, another type of EA which also receive a great attention is electric short take-off and landing aircraft (eSTOL). The research of this kind of EA focuses on method to achieve short take-off and landing distance which may have a relative larger payload and longer cruising distance than eVTOL [11]. As a result, if the runway consumption for eSTOL to take-off and landing may be reduced, it may be able to bring a large amount of cargo to land on some where which the runway distance is restricted such as some small islands. Out of this consideration, in this study, the authors focus on the research of eSTOL to achieve a short landing distance by taking the advantage of fast response time of electric motor and the usage of variable pitch propeller (VPP).

A VPP is a kind of propeller which can change its geometric pitch angle passively or actively and is widely used in modern propeller driven aircraft and helicopter because of its wide thrust variable range and low energy consumption. However, in a conventional propeller driven aircraft, when the counter torque varied abruptly, a vibration of propeller may occur and lead to the instability of the aircraft as a whole because of the

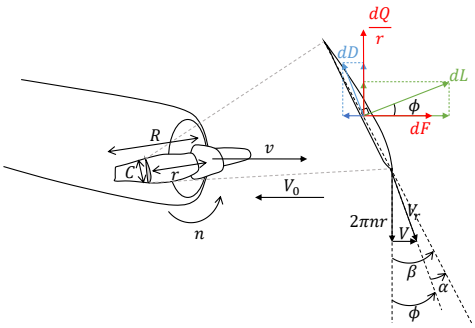

Fig. 1. Blade element model

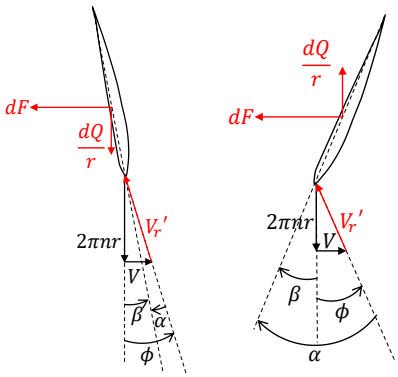

(a) wind-milling brake (b) power-on brake

Fig. 2. Pitch placement at reverse thrust for air brake

low controllability of engine [12]. As a result, a variation of pitch angle through stall region which may have a relatively higher reverse thrust output is not feasible. Where, stall region refers to a range of pitch angle which the propeller can only generate negligible thrust. On the other hand, taking the advantage of the high controllability of motor, the thrust control of EA may be able to become safer [13], and the vibration suppression of counter torque becomes possible, that will make the usage of the full range VPP to be feasible.

In this basic study, the main contribution is to propose and verify the feasibility of a method of using full range VPP to achieve short distance landing for a fixed-wing EA which is considered to be the first study of this region as the author's knowledge. The reverse thrust created by propeller is tested under several pitch angle and a simulation related to the deceleration performance based on the static data measured in the experiment is done to prove the feasibility of using the pitch placement which should transit through the stall region.

II. Propeller Dynamics

A. Blade Element Model

Fig. 1 shows a blade element model for a propeller at the forward thrust pitch placement. R is the radius of the propeller, C is the chord, r is the radius to the blade element, n is rotational speed, β is geometric pitch angle, ϕ is effective pitch angle, α is the angle of attack of propeller, v is advance speed of the propeller, V_0 is the free stream speed, V $(= v + V_0)$ is the relative advance speed of the propeller, V_r is the relative air speed of the propeller, dD is differential drag, dL is differential lift, dQ is differential counter torque, dF is differential thrust. It can be known that the thrust and counter torque created by propeller can be calculated as follow:

$$dF = dL\cos\phi - dD\sin\phi \tag{1a}$$

$$\frac{dQ}{r} = dL\sin\phi + dD\cos\phi \tag{1b}$$

Further, the differential lift dL and drag dD can be calculated as

$$dL = \frac{1}{2}\rho V_r^2 C_L C dr, \tag{2a}$$

$$dD = \frac{1}{2}\rho V_r^2 C_D C dr, \tag{2b}$$

where ρ is air density, C_L is the lift coefficient, C_D is the drag coefficient, dr is differential radius. Combining Eqs. (1) and (2), the total thrust F and total counter torque Q can be calculated as follow:

$$F = \int_0^R \frac{1}{2}\rho V_r^2 C(C_L\cos\phi - C_D\sin\phi)dr \tag{3a}$$

$$Q = \int_0^R \frac{1}{2}\rho V_r^2 C(C_L\sin\phi + C_D\cos\phi)dr \tag{3b}$$

The result of the integration of Eq. (3) can be simplified as

$$F = C_F n^2, \tag{4a}$$

$$Q = C_Q n^2, \tag{4b}$$

where C_F is thrust coefficient, C_Q is counter torque coefficient of the propeller. For a constant rotational speed, because different angle of attack of the propeller may create a different thrust and counter torque, C_F and C_Q may be considered to be the function of ϕ and β. Further, referring to Fig. 1, because the effective pitch angle ϕ can be determined by V and $2\pi nr$, advance ratio J is used in this study to consider the effect of ϕ which is defined as

$$J = \frac{V}{nD_p} \tag{5}$$

where D_p is the diameter of the propeller. As a result, Eq. (4) can be converted to below equations.

$$F = C_F(\beta, J)n^2 \tag{6a}$$

$$Q = C_Q(\beta, J)n^2 \tag{6b}$$

B. Pitch Placement

As it is mentioned in the previous section, a propeller can create different thrust and counter torque at a different angle of attack α. Taking the advantage of it, a VPP has a wide variable range of thrust and have a great performance at the deceleration for an aircraft. Fig. 2 shows two pitch placement for a blade element which creates reverse thrust. In the figure, V_r' is the relative air speed vector for wind to propeller which

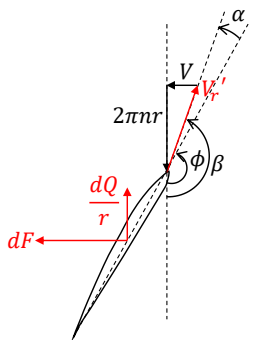

Fig. 3. Back pitch placement at reverse thrust

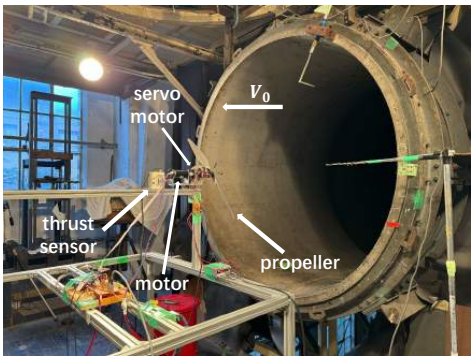

Fig. 4. Experimental setup of VPP test bench

is at the opposite direction of V_r. It can be known that reverse thrust may establish while the relative air speed vector goes into the propeller at the forward surface of propeller. That is, the propeller may also create reverse thrust at the pitch placement as it is shown in Fig. 3.

Under this situation, different from the situation of Fig. 2 which the direction of wind flow go through the propeller is as the same as free stream, propeller's relative advance speed V is reversed because of the reversal of wind flow go through the propeller. Thus, it have a particular direction of $V_r^{'}$. This phenomenon will be described in Section. III-D in detail by using experimental results. In order to have a better reference to these pitch placement, in this study, the pitch placement of Fig. 1 is named as forward pitch (FP). Fig. 2(a) is ignored because of the narrow range of this pitch placement, the pitch placement of Fig. 2(b) is named as reverse pitch (RP) and the pitch placement of Fig. 3 is named as back pitch (BP). Further, β will be considered to be positive at FP and BP, negative at RP and to be $0°$ at the same direction of rotational speed.

C. Rotational Motion of Propeller

The rotational motion of the propeller is shown as follow:

$$J_\omega \dot{\omega} = K_t I - B_\omega \omega - Q \tag{7}$$

where, J_ω is inertia of propeller, K_t is torque constant, B_ω is viscosity coefficient of propeller, ω is the angular velocity of propeller and Q is counter torque. J_ω, K_t and B_ω are measured in previous study [14].

III. Experiment for Parameter Identification

A. Experiment Objective

The purpose of this experiment is to measure the thrust coefficient C_F and counter torque coefficient C_Q of the pitch placement at forward, reverse and back. Furthermore, the wind flow goes through the propeller while at the BP is measured qualitatively to aid the research in the future.

B. Experimental Setup

Fig. 4 shows experiment setup in the low speed wind tunnel. The propeller utilized in the experiment is APC propeller $20\times13E$ which was modified to VPP. Because of the washout of propeller, the geometric pitch angle β is measured at the center of the propeller. The experiment is conducted in several different constant free stream wind speed V_0, while changing the geometric pitch angle and rotational speed. The thrust F and counter torque Q created by the propeller is measured by the thrust sensor and torque current I, respectively. The counter torque is calculated based on the constant angular velocity input of ω as,

$$Q = K_T I - B_\omega \omega. \tag{8}$$

Using the measured value from experiment, C_F and C_Q can be calculated by Eqs. (6) and (8).

C. Experiment Results and Function Fitting for C_F and C_Q

The experiment results of C_F and C_Q are shown in Figs. 6 and 7. Because of the limitation of mechanism of the test bench in this experiment, the dynamic characteristic during the transition of the pitch angle cannot be obtained, which will be taken in future work using new types of VPP mechanism. Furthermore, the data can only be taken in a range of the geometric pitch angle β within $-25°$ to $20°$ and $150°$ to $180°$. Further, in order to express the overall tendency of C_F and C_Q, a function fitting is also done and shown in experiment results. The fitting method used in this study is expressed as follow. The fitting functions for C_F and C_Q are shown as

$$C_F,\ C_Q = \sum_{i=0}^{p} a_{p-i}(\beta) J^{p-i}, \tag{9a}$$

$$a_{p-i}(\beta) = \sum_{j=0}^{q} b_{(p-i)j} \beta^j. \tag{9b}$$

Considering the characteristics from J to C_F or C_Q [6] and data measured in the experiment, C_F and C_Q are fitting as a first order function of J at Eq. (9a). Furthermore, the geometric pitch angle β fitness n at Eq. (9b) can be referred to Eqs. (3) and below equations as

$$C_L = a_{L1}\alpha + a_{L2}, \tag{10a}$$

$$C_D = a_{D2}\alpha^2 + a_{D1}\alpha + a_{D0}, \tag{10b}$$

where a is the propeller parameter for lift and drag. While the free stream speed is low and the geometric pitch angle β is small, angle of attack α can be approximated to β and

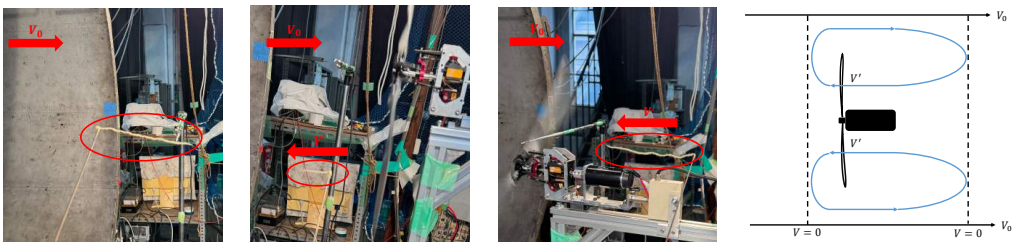

(a) Free stream (b) Wind flow through propeller (front) (c) Wind flow through propeller (back) (d) Image of wind flow

Fig. 5. Wind flow through propeller while at the back pitch placement

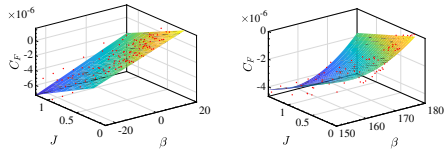

(a) FP and RP (b) BP

Fig. 6. C_F of several pitch placement

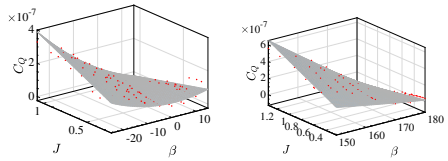

(a) FP and RP (b) BP

Fig. 7. C_Q of several pitch placement

the allocation of drag in thrust shows a first order function to β. While β goes up and not reach the stall region yet, the allocation of drag in thrust becomes larger and the second order function shows up at the function of thrust to geometric pitch angle. As a result, for the data of FP and RP, a first order approximation related to β is used, and for the data of BP, a second order approximation related to β is used. Further, C_Q can be fitted to a second order function to β in all pitch placement using the same method.

D. Wind Flow of Back Pitch Placement

As it is mentioned in the previous section, the air flow goes through the propeller from the same direction in the FP and RP conditions. However, at the BP placement, the air flow direction going through the propeller is at the opposite direction as to the free stream. The experimental result to confirm the direction of air flow is shown in Fig. 5. In this experiment, the parameters are set as $n = 1600\,\mathrm{rpm}$, $\beta = 170°$, $V_0 = 3.34\,\mathrm{m/s}$. The free stream air flow V_0 is from left to right which is shown in Fig. 6(a), but the motion of tuft shows that the wind flow through the propeller $V^{'}$ is from right to left which means that the propeller is pushing the air forward to establish the reverse thrust which is shown in Fig. 5(d). As a result, it can be confirmed that the reverse thrust achieved by the transition of pitch angle from forward to back is practically limited by a stall region which stems from the reversal and reattachment of the air flow.

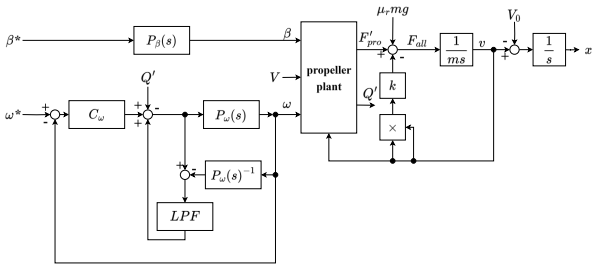

Fig. 8. Simulation block diagram

TABLE I
PARAMETERS USED IN THE SIMULATION

Symbol	Definition	Value	Unit
m	Mass of aircraft	2	kg
v	Relative airspeed of aircraft	–	$\mathrm{m\,s^{-1}}$
k	air resistance constant	0.0303	–
μ_r	Rotational friction coefficient	0.01	–
g	Gravitational acceleration	9.81	$\mathrm{m\,s^{-2}}$
ρ	Air density	1.2	$\mathrm{kg\,m^{-3}}$
S	Surface area of wings	0.5	$\mathrm{m^3}$
C'_D	Drag coefficient of wings	0.101	–

IV. Simulation of Aircraft Landing

A. Simulation Setup

In order to compare the deceleration efficiency of the reverse thrust produced by propeller at reverse and back pitch angle placement, a simulation is conducted in this section on a simplified single-propeller aircraft model. In this paper, we only focus on the longitudinal motion, which is shown as follows:

$$m\frac{dv}{dt} = C_F(\beta, J)n^2 - kv^2 - \mu_r mg \tag{11a}$$

$$k = \frac{1}{2}\rho S C'_D \tag{11b}$$

The values and definition of parameters used in the simulation in Eq. (11) are listed in Table I, which partly uses the values in previous study [15]. The block diagram used in this

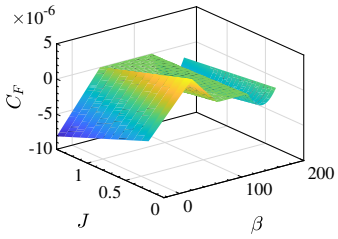

Fig. 9. Fitting function for BP based on the assumptions

simulation is shown in Fig. 8. Geometric pitch angle β and angular velocity ω is used as the control input. The angular velocity control system involved a P control and a disturbance observer (DOB). The nominal transfer function from motor torque to propeller rotational speed is

$$P_\omega(s) = \frac{K_T}{J_\omega s + B_\omega} \tag{12}$$

The geometric pitch angle model uses first order delay system. Eq. (6) is used in propeller plant and the coefficient of thrust and counter torque is calculated based on the fitting functions obtained in the experiments as shown in Fig. 6 and 7.

B. Assumptions for Simulation

Because of the limitation of VPP test bench used in the experiment, following assumptions related to C_F are made to complement the data between $15°$ and $150°$ and the fitting function based on it is shown in Fig. 9.

- The aerodynamics within this region related to the hysteresis of thrust response caused by the stall of propeller and the delay of the airplane response to the thrust response is ignored because of the lack of data. Further, the lift created by wings is considered to be negligible and the influence of it to normal force is ignored.
- With the increase of β at forward pitch placement, the forward thrust will reach a peak and goes down refers to Eq. (3) and be stall because of the reversal of wind flow go through the propeller. The data from $-20°$ to $45°$ is based on the fitting function of reverse and forward pitch, the data from $45°$ to $90°$ used the symmetric fitting function at the pitch angle of $30°$ as the same trend of the region between $-20°$ to $30°$. In order to simulate the stall of propeller during the transition from forward to back, C_F is set as 0 when the value is lower than 0 following the line trend from $45°$.
- The data between $90°$ to $180°$ used the fitting function for BP as shown in Fig. 6(b). Furthermore, if C_F is higher than 0, it will be considered as 0 in this region.

C. Simulation Results

The simulation is conducted to validate the effectiveness of bp compared to RP on MATLAB/Simulink 2024a based on assumptions made in the previous section. The initial position is $10°$ and the target position of the transition for reverse pitch and back pitch is $\beta = -10°$ and $170°$ respectively. Rotational speed is $n = 1600\,\mathrm{rpm}$, free stream velocity is $V_0 = 1\,\mathrm{m/s}$. The deceleration starts at the relative airspeed of $v = 10.7\,\mathrm{m/s}$. By changing the control input of pitch angle β, the performance of reverse thrust of RP and BP is compared in this study.

The pitch angle is input as a step and responds as a first-order delay with a time constant of $0.05\,\mathrm{s}$. The result is shown in Fig. 10. During the transition from FP to BP, propeller will create larger thrust at first and then go down. Referring to the assumption made in previous section, it may also have a stall region during the transition. Furthermore, since the assumption cannot completely represent the characteristics of C_F, the rotational speed response of BP have a response shown in Fig. 10(b). Under this condition, the landing distance is shortened by approximate $30\,\%$ by using the BP.

Furthermore, considering the constraints of the transition speed of pitch angle of VPP mechanism, the pitch angle is also inputted as a ramp in this study. As it is shown in Fig. 11, while the pitch angle input gradient is $180\,°/\mathrm{s}$, using BP can have an approximate $5\,\%$ shorten of landing distance. However, referring to Fig. 12, which the pitch angle is inputted as $120\,°/\mathrm{s}$ ramp, conventional method with RP may have a shorter landing distance. This is because firstly a lower transition speed of pitch angle lead to a longer time for blade to stay at the stall region, and secondly a longer time to make the aircraft accelerate at the pitch angle range between $10°$ and $45°$.

Based on the simulation results, it can be concluded that, using BP may achieve a relative short landing distance. However, the constraint of blade angle travel speed may also limit the performance of it. In future work, changing the input of geometric pitch angle β and angular velocity ω to the input of thrust may restrict the acceleration part of the transition to BP. Further, reducing the effect of the stall of propeller may also enhance the feasibility of using BP.

V. Conclusion and Future Work

In this basic study, a relatively larger reverse thrust pitch placement for a VPP is proposed and an experiment is conducted to verify it. Comparing with the conventional use of VPP at RP, proposal method of using BP have a relatively larger reverse thrust and may be able to have a shorter landing distance which is verified by a simulation used the data measured in the experiment. To enhance the feasibility of the proposed method, following future works should be considered and conducted.

- A new mechanism for VPP which may have a full scale variable range should be proposed in order to take the data which was not been taken in this study.
- Because of the stall of propeller during the transition to BP, a sudden change of torque may occur and lead to an unstable response of angular velocity with vibration. As a result of the lack of data, the simulation of the control of torque vibration for rotational control system which take the advantage of high controllable ability of electric

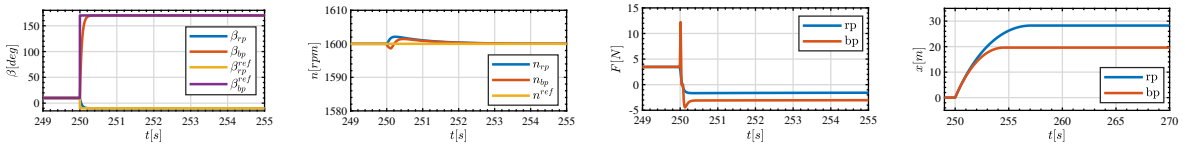

(a) Pitch angle response (b) Rotational speed response (c) Thrust response (d) Landing distance

Fig. 10. Response of step input of pitch angle

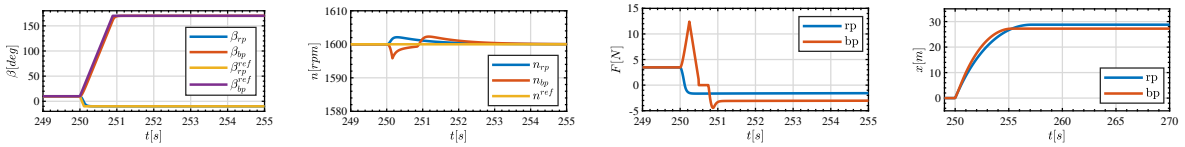

(a) Pitch angle response (b) Rotational speed response (c) Thrust response (d) Landing distance

Fig. 11. Response of 180 °/s ramp input of pitch angle

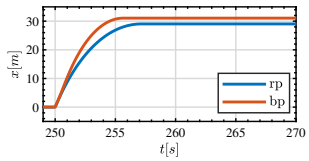

Fig. 12. Landing distance of 120 °/s ramp input of pitch angle

motor was not done in this study and will be finished on new test bench.

- The transient trait regarding aerodynamics between the stall region during the transition was ignored in this study which may limit the feasibility of using BP. It will be measured using the new mechanism VPP, and the proposal to eliminate or reduce its effect will also be considered and established in future study.
- The target control system have a control input of thrust. However, because of the lack of data, the simulation done in this study used geometric pitch angle β and angular velocity ω for the control input. The optimization of control input distribution will be proposed in future work. Further, the pitch angle control system may also be changed in order to meet the demand of the overall control system.
- Optimal speed trajectory generation will be made for further future work. At last, a demonstration experiment will be made on a small scale radio controlled electric aircraft to verify the total proposed methods.

ACKNOWLEDGMENT

This work was partly supported by JSPS KAKENHI Grant Number JP23H00175, Japan.

REFERENCES

[1] P. J. Ansell and K. S. Haran, "Electrified airplanes: A path to zero-emission air travel," *IEEE Electrification Magazine*, vol. 8, no. 2, pp. 18–26, 2020.

[2] Y. Hori, "Future vehicle driven by electricity and control-research on four-wheel-motored "UOT electric march II"," *IEEE Transactions on Industrial Electronics*, vol. 51, no. 5, pp. 954–962, 2004.

[3] A. Norihiko, K. Hiroshi, H. Hideaki, and N. Akira, "An experimental study on energy regeneration using propellers," *JAXA-RR-*, no. 15-001, p. 170, 2015.

[4] S. Yamamoto and H. Hirahara, "Torque estimation of variable-speed induction motors without torque and rotational speed meters," *IEEJ Journal of Industry Applications*, vol. 13, no. 3, pp. 233–242, 2024.

[5] D. Golovanov, D. Gerada, G. Sala, M. Degano, A. Trentin, P. H. Connor, Z. Xu, A. L. Rocca, A. Galassini, L. Tarisciotti, C. N. Eastwick, S. J. Pickering, P. Wheeler, J. Clare, M. Filipenko, and C. Gerada, "4-mw class high-power-density generator for future hybrid-electric aircraft," *IEEE Transactions on Transportation Electrification*, vol. 7, no. 4, pp. 2952–2964, 2021.

[6] K. Yokota and H. Fujimoto, "Pitch angle control by regenerative air brake for electric aircraft," *IEEJ Journal of Industry Applications*, vol. 11, no. 2, pp. 308–316, 2022.

[7] L. A. Garrow, B. J. German, and C. E. Leonard, "Urban air mobility: A comprehensive review and comparative analysis with autonomous and electric ground transportation for informing future research," *Transportation Research Part C: Emerging Technologies*, vol. 132, p. 103377, 2021.

[8] E. C. Suiçmez and A. T. Kutay, "Full envelope nonlinear flight controller design for a novel electric VTOL (eVTOL) air taxi," *The Aeronautical Journal*, vol. 128, no. 1323, pp. 966–993, 2024.

[9] B.-M. Nguyen, T. Kobayashi, K. Sekitani, M. Kawanishi, and T. Narikiyo, "Altitude control of quadcopters with absolute stability analysis," *IEEJ Journal of Industry Applications*, vol. 11, no. 4, pp. 562–572, 2022.

[10] S. Shahjahan, A. Gong, A. Moore, and D. Verstraete, "Optimisation of proprotors for tilt-wing evtol aircraft," *Aerospace Science and Technology*, vol. 144, p. 108835, 2024.

[11] C. Courtin, A. Mahseredjian, A. J. Dewald, and J. Hansman, "A performance comparison of eSTOL and eVTOL aircraft," in *AIAA AVIATION 2021 FORUM*, 2021.

[12] E. T. Duran, "Methodology for counter torque, power loss, and frictional heat for brush seals under eccentric transients," *Tribol. Trans.*, vol. 66, no. 2, pp. 249–267, 2023.

[13] K. Takahashi, H. Fujimoto, Y. Hori, H. Kobayashi, and A. Nishizawa, "Modeling of propeller electric airplane and thrust control using advantage of electric motor," *IEEE 13th International Workshop on Advanced Motion Control (AMC), 482-487*, 2014.

[14] Y. Naoki, S. Nagai, and H. Fujimoto, "Mode-switching algorithm to improve variable-pitch-propeller thrust generation for drones under motor current limitation," *IEEE/ASME Transactions on Mechatronics*, vol. 28, no. 4, pp. 2003–2011, 2023.

[15] T. Katagiri, K. Yokota, K. Fujimoto, S. Nagai, and H. Fujimoto, "Basic study on velocity control in wing coordinate system using acceleration-based disturbance observer for tilt-wing evtol," in *The 10th IEEJ international workshop on Sensing, Actuation, Motion Control, and Optimization*, 2023.